

White-matter functional networks changes in patients with schizophrenia

Yuchao Jiang^a, Cheng Luo^{a,*}, Xuan Li^a, Yingjia Li^a, Hang Yang^a, Jianfu Li^a, Xin Chang^a,
Hechun Li^a, Huanghao Yang^a, Jijun Wang^b, Mingjun Duan^{a,c}, Dezhong Yao^{a,**}

^a The Clinical Hospital of Chengdu Brain Science Institute, MOE Key Lab for Neuroinformaton, Center for Information in Medicine, School of Life Science and Technology, University of Electronic Science and Technology of China, Chengdu, 610054, China

^b Shanghai Key Laboratory of Psychotic Disorders, Shanghai Mental Health Center, Shanghai Jiaotong University School of Medicine, Shanghai, 200030, China

^c Department of Psychiatry, Chengdu Mental Health Center, Chengdu, 610054, China

ARTICLE INFO

Keywords:

White-matter functional network
Schizophrenia
Resting-state functional connectivity
fMRI

ABSTRACT

Resting-state functional MRI (rsfMRI) is a useful technique for investigating the functional organization of human gray-matter in neuroscience and neuropsychiatry. Nevertheless, most studies have demonstrated the functional connectivity and/or task-related functional activity in the gray-matter. White-matter functional networks have been investigated in healthy subjects. Schizophrenia has been hypothesized to be a brain disorder involving insufficient or ineffective communication associated with white-matter abnormalities. However, previous studies have mainly examined the structural architecture of white-matter using MRI or diffusion tensor imaging and failed to uncover any dysfunctional connectivity within the white-matter on rsfMRI. The current study used rsfMRI to evaluate white-matter functional connectivity in a large cohort of ninety-seven schizophrenia patients and 126 healthy controls. Ten large-scale white-matter networks were identified by a cluster analysis of voxel-based white-matter functional connectivity and classified into superficial, middle and deep layers of networks. Evaluation of the spontaneous oscillation of white-matter networks and the functional connectivity between them showed that patients with schizophrenia had decreased amplitudes of low-frequency oscillation and increased functional connectivity in the superficial perception-motor networks. Additionally, we examined the interactions between white-matter and gray-matter networks. The superficial perception-motor white-matter network had decreased functional connectivity with the cortical perception-motor gray-matter networks. In contrast, the middle and deep white-matter networks had increased functional connectivity with the superficial perception-motor white-matter network and the cortical perception-motor gray-matter network. Thus, we presumed that the disrupted association between the gray-matter and white-matter networks in the perception-motor system may be compensated for through the middle-deep white-matter networks, which may be the foundation of the extensively disrupted connections in schizophrenia.

Introduction

Although traditional structural techniques, such as diffusion-tensor imaging (DTI), can successfully explore the details of white-matter structural architecture, they fail to uncover neural activity and relevant functions that occur inside white-matter. Over the past two decades, resting-state functional MRI (fMRI), which is based on blood oxygen level-dependent (BOLD) signals, has been a useful technique for investigating the functional organization of human gray-matter in cognitive neuroscience and clinical neuropsychiatry (Biswal et al., 1995; Meda et al., 2014). However, it has limited use for evaluating the functional

organization of the cerebral white-matter since white-matter has very few postsynaptic potentials that give rise to BOLD signals (Logothetis et al., 2001). Recently, accumulated works have found that the functional activity in white-matter corresponds to related demands in multiple tasks, including perceptual, language and motor tasks (Fabri and Polonara, 2013; Fabri et al., 2011; Gawryluk et al., 2011, 2014). These studies demonstrated the existence of functional brain activity in the white-matter, and suggested that the functional information from white-matter can be detected by fMRI.

Recently, the functional organization of white-matter in resting-state has received greater attention (Ding et al., 2018; Ji et al., 2017;

* Corresponding author. University of Electronic Science and Technology of China, Second North Jianshe Road, Chengdu, 610054, China.

** Corresponding author. University of Electronic Science and Technology of China, Second North Jianshe Road, Chengdu, 610054, China.

E-mail addresses: chengluo@uestc.edu.cn (C. Luo), dyao@uestc.edu.cn (D. Yao).

<https://doi.org/10.1016/j.neuroimage.2018.04.018>

Received 21 November 2017; Received in revised form 26 March 2018; Accepted 9 April 2018

Available online 13 April 2018

1053-8119/© 2018 Elsevier Inc. All rights reserved.

Marussich et al., 2017; Mezer et al., 2009). For example, Ji and colleagues observed the power of resting-state BOLD signals associated with white-matter density and fractional anisotropy (Ji et al., 2017). Marussich and colleagues evaluated white-matter functional connectivity and found that fMRI carried functional information about white-matter activity and connectivity at rest (Marussich et al., 2017). In addition, Peer and colleagues clustered all the white-matter voxels into several functional networks in a cluster analysis and found a correspondence between white-matter and gray-matter functional networks as well as DTI tracts (Peer et al., 2017), further suggesting the intrinsic functional organization of white-matter. Previous studies provided evidences of the existence of white-matter functional networks, and examined their reliability and reproducibility in healthy controls. However, most importantly, few study investigated white-matter functional networks in patients with brain disorders. Many brain disorders, including schizophrenia, epilepsy, Alzheimer's and Parkinson's disease, are characterized by white-matter abnormalities (Bohnen and Albin, 2011; Caso et al., 2015; Dong et al., 2017a; Xue et al., 2014). Therefore, it is important to explore the altered white-matter functional networks in these disorders, and this also contributes to the understanding of psychiatric pathological mechanisms on neuroimage (Kressel, 2017; Lui et al., 2016).

Schizophrenia has been hypothesized to be a psychiatry disorder involving insufficient or ineffective communication between large-scale functional networks and cortical-subcortical pathways (Chen et al., 2017; Dong et al., 2017b; Duan et al., 2015; Friston, 1998; Huang et al., 2017; Jiang et al., 2017). Morphometric studies have revealed gray-matter volume atrophy in the cortices and subcortical regions in schizophrenia (Jiang et al., 2018). As white-matter is composed of densely myelinated axons interconnecting gray-matter regions, abnormalities of white-matter have long been proposed to be possible factors in the pathophysiology of schizophrenia (Burns et al., 2003). Accumulated studies have frequently implicated alterations in white-matter tracts in schizophrenia using DTI (Holleran et al., 2014; Karlsgodt et al., 2008; Smith et al., 2006). In the functional aspect, previous PET studies showed relatively increased glucose metabolic rate in white-matter in schizophrenia (Buchsbaum et al., 2007). However, few functional study in schizophrenia uncovered dysfunctional connectivity within the white-matter. In this study, large-scale white-matter functional networks were characterized by applying a cluster analysis to the resting-state fMRI data of white-matter in a large cohort of patients with schizophrenia (N = 97) and healthy controls (N = 126). We estimated the functional connectivity within the resulting white-matter functional networks and their relationship to the known gray-matter functional networks. In addition, we investigated the spontaneous activity within the white-matter functional networks. By comparing the differences in the white-matter functional networks between patients with schizophrenia and healthy controls, this study linked the white-matter functional abnormalities with the pathophysiology of schizophrenia.

Material and methods

Participants

This study included ninety-seven patients with schizophrenia (gender: 68 males and 29 females; age: 41 ± 11.5 years) and 126 healthy controls (gender: 84 males and 42 females; age: 38 ± 14.9 years) matched to the patient group by age and gender. According to the Diagnostic and Statistical Manual of Mental Disorders, Fourth Edition (DSM-IV), each patient was diagnosed at the Clinical Hospital of Chengdu Brain Science Institute. Subjects with a history of brain injuries, substance-related disorders, and major medical or neurological disorders were excluded. All schizophrenia patients were taking antipsychotics medication. The chlorpromazine equivalent dose of the antipsychotics was 324.5 ± 157.1 mg/day. Positive and Negative Syndrome Scale (PANSS) was used to assess the symptom severity. Healthy controls with a history of psychiatric disorder in a first- or second-degree relative were

also excluded due to the potential genetic effects. The study was approved by the Ethics Committee of the Clinical Hospital of Chengdu Brain Science Institute, and written informed consent was obtained from all the subjects.

Image acquisition

Imaging data were collected using a 3-T MRI scanner (GE DISCOVERY MR 750, USA) at the University of Electronic Science and Technology of China. High-resolution T1-weighted images were acquired by a three-dimensional fast spoiled gradient-echo (T1-3D FSPGR) sequence. The main scanning parameters were as follows: repetition time (TR), 6.008 ms; echo time (TE), 1.984 ms; flip angle, 90°; field of view, 25.6 cm × 25.6 cm; matrix size, 256 × 256; and slice thickness, 1 mm (no gap). Resting-state functional images were acquired using a gradient-echo echo-planar imaging (EPI) sequence. The main scanning parameters were as follows: TR, 2s; TE, 30 ms; flip angle, 90°; field of view, 24 cm × 24 cm; matrix size, 64 × 64; slice thickness, 4 mm (no gap), slice number, 35; and scanning time, 510 s (255 vol). Participants were instructed to remain awake, close their eyes, and try not to think of anything. All the subjects confirmed that they did not fall asleep during scans.

Data preprocessing

T1 images were segmented into white-matter, gray-matter and cerebrospinal fluid (CSF) using *SPM8's New Segment algorithm* and then normalized to the MNI template. The functional image preprocessing steps included the following. (1) The first five time points were removed for signal equilibrium and to allow the participants to adapt at to the scanning noise. (2) Slice-time correction. (3) Realignment to the mean functional image was performed using a trilinear interpolation with degrees of freedom and coregistered with the anatomical image. Subjects with maximum motion >2 mm or 2° were excluded. (4) Removal of linear trends to correct for signal drift. (5) Nuisance signal (including 24-parameter motion correction and the mean CSF signals) was regressed out. The 24 motion parameters included six rigid-body motion parameters (x, y and z translations and rotations) and their values at the previous time point and the 12 corresponding squared values. The white-matter and global brain signals were not regressed out because this could have eliminated signals of interest. (6) Temporal scrubbing using motion “spikes” (framewise displacement (FD) > 1) as separate repressors was performed. The scrubbing effectively censored the data at the spike without further changing the correlation values. (7) Band-pass filtering (0.01–0.15 Hz) was performed to reduce non-neuronal contributions to BOLD fluctuations. (8) To avoid mixing white-matter and gray-matter signals, spatial smoothing was performed separately on the white-matter or gray-matter masks. In detail, the individual T1 segmentation images were coregistered to the functional space for each participant for the identification of white-matter or gray-matter masks (the threshold was set at 0.5). The individual functional images were smoothed (FWHM = 4 mm) separately on the two masks. Finally, we used only the smoothed data from the white-matter mask. (9) Normalization to the standard EPI template and resampling to 3 mm³ voxels were performed. Steps 1–8 were performed on each subject's original sampling space in order to distinguish white-matter and gray-matter signals at the individual level. Preprocessing was performed using SPM12 (www.fil.ion.ucl.ac.uk/spm/), DPABI (<http://rfmri.org/dpabi>) and open MATLAB scripts (<http://mind.huji.ac.il/white-matter.aspx>). After motion-correction, 93 schizophrenia patients and 125 healthy controls were included in this study. As a previous study reported that even slight head-motion could lead to increased long-range connectivity, we examined group-level head-motion differences between the schizophrenia patient group and healthy control group using the two-sample *t*-test. In addition, group-level statistical analysis showed no difference (Supplementary 1).

Clustering white-matter networks in the white-matter mask

The analysis pipeline was similar to the original study by Peer and colleagues (Peer et al., 2017) and is briefly described here. To obtain unified white-matter and gray-matter masks at the group-level, we used the T1 image segmentation results. For each subject, we identified each voxel as white-matter, gray-matter or CSF based on its maximum probability from the segmentation results. This resulted in individual white-matter, gray-matter and CSF masks. These masks were averaged across all the subjects, and the percentage of subjects that were classified as white-matter or gray-matter were obtained. For white-matter, the voxels with a percentage >60% were identified as the group-level white-matter mask. We also applied two stricter masks (percentages > 70% and 80%) to obtain the group-level white-matter mask (Supplementary 2). Then, the subcortical areas based on the Harvard-Oxford Atlas (Desikan et al., 2006) were removed from the white-matter mask to correctly classify the deep brain structures (Lorio et al., 2016). Finally, the T1 white-matter mask was coregistered to the functional space and resampled for functional image processing. In addition, for gray-matter, a loose threshold of percentage >20% was used to identify as white-matter mask containing almost all the gray-matter voxels.

Considering the computational complexity, an interchanging grid strategy was used to subsample 18,591 voxels in the white-matter mask to 4,623 nodes (Craddock et al., 2012). In detail, any second voxels along the rows and columns were taken and then shifted by 1 between the two slices. Pearson's correlation coefficients between each white-matter voxel and subsampled node were computed and resulted in a correlation pattern ($18,591 \times 4,623$ matrix) for each subject. An identified clustering approach was used to determine the white-matter networks. K-means clustering (distance metric-correlation, 10 replicates) was performed on the averaged correlation matrices. As the clustering was performed on the whole group of unequal numbers of patients and controls, the clustering results may be more heavily weighted to the controls and lead to bias. The correlation matrix was first averaged across each group of subjects and then averaged again across the two groups. To obtain the most stable number of networks, the numbers of clusters ranging from 2 to 22 and the stability were measured for each cluster number according to previously described methods (Buckner et al., 2011). We randomly divided the whole connectivity matrix ($18,591 \times 4,623$) into four folds ($18,591 \times 1,155$). For each number of clusters, the same clustering computation was performed on each fold separately. To measure the similarity between the clustering in different folds, an adjacency matrix was calculated and then compared using Dice's coefficient. The averaged Dice's coefficient was used to assess the stability of the number of clusters.

Functional connectivity of white-matter networks

To measure the functional connectivity between individual white-matter networks, we extracted the average time courses from all ten white-matter networks by averaging across all voxels belonging to one network for each subject. The Pearson's correlation between the average time courses of any two white-matter networks was computed for each subject and transformed to the Fisher z score for the statistical analysis. In addition, to measure the relationship between white-matter and gray-matter networks, we also calculated the Pearson's correlation coefficient between each white-matter network and gray-matter network. These correlation coefficients were averaged across subjects to obtain the group-level matrix that represented the relationship between white-matter and gray-matter networks. Considering that many studies showed reliable and reproducible clustering results using gray-matter signals (Power et al., 2011; Shirer et al., 2012), this study did not cluster the gray-matter networks but used a previously obtained gray-matter network atlas that was generated by the same clustering procedure for the gray-matter voxels. The gray-matter network atlas closely

corresponded to the cortical network subdivisions (Buckner et al., 2011; Power et al., 2011; Yeo et al., 2011). The two-sample *t*-test was performed on the z-score of Pearson's correlation coefficient to show the differences between the schizophrenia and healthy control groups ($P < 0.05$, Bonferroni corrected).

Spontaneous activity of white-matter networks

The spontaneous low frequency fluctuations of BOLD signal in the resting state have been identified as biological measures of baseline spontaneous activity (Fox and Raichle, 2007). In this study, signal amplitudes in each frequency were calculated using the Fourier transform (MATLAB's FFT function) for each white-matter network of each subject (Supplementary 3). The resulting frequency graphs were separately averaged across subjects in the schizophrenia and healthy control groups for each network. Considering that the spontaneous oscillatory amplitudes in the different frequency bands may reflect distinct neural activities and physiological states (Meda et al., 2015; Yu et al., 2014), we further divided the whole band (band A: 0.01–0.15 Hz) into two sub-bands (band B: 0.08–0.15 Hz; band C: 0.01–0.08 Hz). For each white-matter network and sub-band, the averaged amplitude was obtained in each subject and then used to compare the differences between the schizophrenia and healthy control groups using ANOVA.

Correlations between altered white-matter networks and clinical variables

We further investigated the relationships between clinical variables (disease duration and PANSS scores) and altered functional connectivity as well as low frequency spontaneous fluctuations. The Pearson's correlation analyses were performed for the schizophrenia group controlling for the effect of antipsychotic medications (chlorpromazine equivalent dose of the antipsychotics). In addition, we also investigated the relationship between the effect of antipsychotic medications and white-matter network functional indices.

Analysis for the potential influence of gray-matter signals

Although this study was cautious in its data analysis, such as smoothing the white-matter and gray-matter separately and preprocessing in individual spaces, it is still of concern whether the correlation or clustering pattern of the white-matter fMRI signals were simply due to the leakage of the gray-matter fMRI signal, particularly with regard to the partial volume effect. We provided several ways to evaluate the potential influence of gray-matter signals as much as possible and re-examined the consistency of the results. First, a relatively stricter mask was applied to identify white-matter voxels (Supplementary 2). Second, the correlations between the different white-matter clusters after regressing out the gray-matter signals were examined (Supplementary 4). Finally, we also evaluated the effects of spatial distance between the white-matter and gray-matter networks (Supplementary 5).

Results

White-matter functional networks

To identify white-matter functional networks with distinct connectivity profiles, we adopted a clustering approach based on white-matter resting-state voxel-wise correlation matrices. Dice's coefficient showed that the most stable segregation number was ten (Supplementary 6); thus, we applied ten networks to conduct following analyses. Consistent with the previous study (Peer et al., 2017), the K-means clustering method identified a symmetrical, interlaced pattern of functional networks inside the white-matter areas that was divided into three layers (superficial, middle and deep) (Fig. 1). The detailed information regarding the ten networks is presented in Table 1.

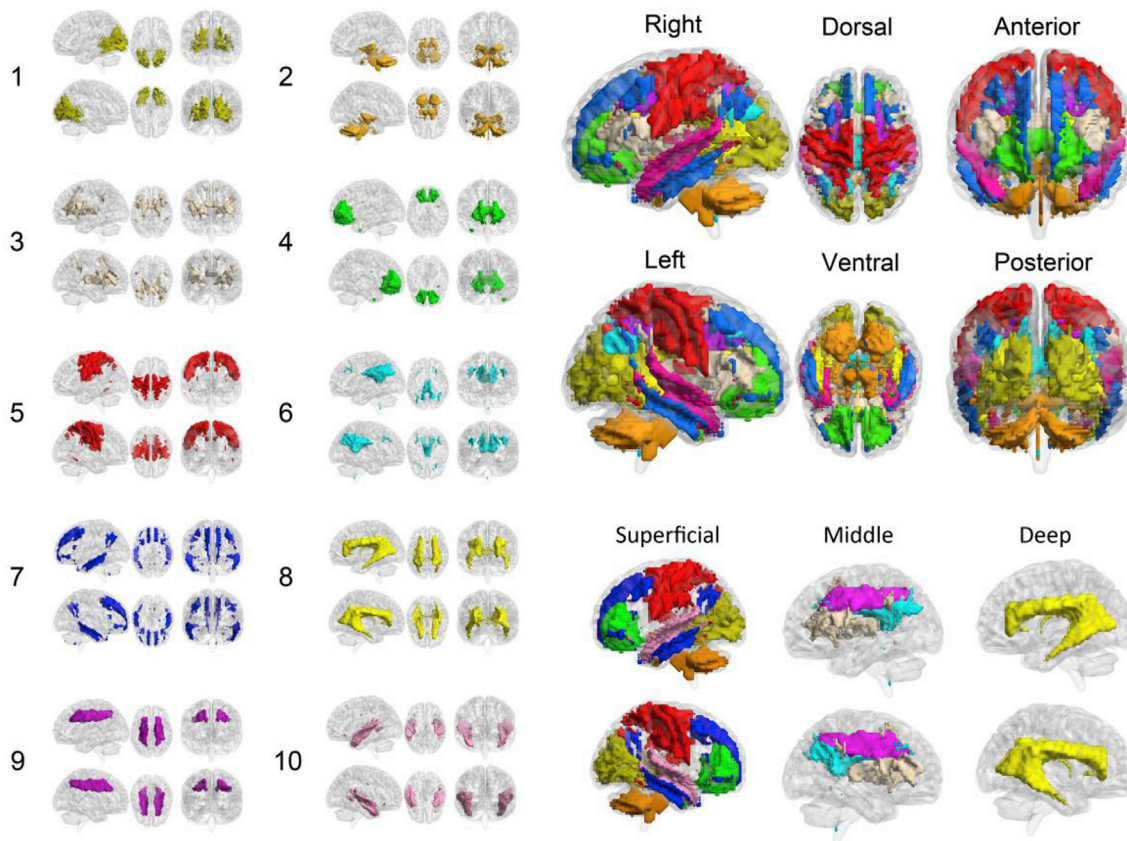


Fig. 1. White-matter functional networks. 1. Occipital network; 2. Cerebellar network; 3. Anterior corona radiate network; 4. Orbitofrontal network; 5. Pre/post-central network; 6. Posterior callosum network; 7. Tempofrontal network; 8. Deep network; 9. Superior corona radiate network; 10. Superior temporal network.

Table 1
White-matter functional networks.

Number	White-matter network	Layer	Correlation with gray-matter network (r value)
1	Occipital network	Superficial	Visual network (0.94)
2	Cerebellar network	Superficial	Cerebellum anterior network (0.83)
3	Anterior corona radiate network	Middle	Dorsal attention network (0.79)
4	Orbitofrontal network	Superficial	Ventral attention network (0.61)
5	Pre/post-central network	Superficial	Sensori-motor network (0.90)
6	Posterior callosum network	Middle	Default-mode network (0.70)
7	Tempofrontal network	Superficial	Default-mode network (0.90)
8	Deep network	Deep	Cerebellum posterior network (0.49)
9	Superior corona radiate network	Middle	Dorsal attention network (0.62)
10	Superior temporal network	Superficial	Sensori-motor network (0.73)

Functional connectivity within white-matter networks

To investigate the relationship among individual white-matter networks, we measured the functional connectivity between any two white-matter networks (Fig. 2a). Two sample t-tests revealed that compared with the healthy control group, the schizophrenia group showed increased functional connectivity between the occipital network and the cerebellar, anterior corona radiate, posterior callosum and deep networks (Table 2 and Fig. 2b). In addition, the schizophrenia group exhibited increased functional connectivity between the pre/post-central network and the anterior corona radiate,

posterior callosum, superior corona radiate and deep networks (Table 2 and Fig. 2b).

Functional connectivity between white-matter networks and gray-matter networks

To examine the relationship between white-matter and gray-matter networks, we also quantified the correlation using the functional connectivity between each white-matter network and all the gray-matter networks (Fig. 2c). Specific white-matter networks exhibited highly functional connectivity ($r > 0.8$) with gray-matter networks (Table 1). In particular, some superficial networks, such as the occipital, cerebellar, orbitofrontal, pre/post-central and tempofrontal networks, were mostly correlated to their overlying gray-matter networks, which may suggest a role of close-range communications within these networks. The correlation between two distant networks was considered to be long-range communication. In addition, the deep networks were weakly correlated to all the gray-matter networks. Comparisons between the schizophrenia and healthy control groups showed decreased functional connectivity between the white-matter occipital network and the gray-matter visual network, the white-matter orbitofrontal network and the gray-matter temporal-orbitofrontal network, and the white-matter superior temporal network and the gray-matter ventral attention network in the schizophrenia group (Table 3 and Fig. 2d). There was some increase in functional connectivity between the occipital, pre/post-central and cerebellar networks in the schizophrenia group (Table 3 and Fig. 2d).

Spontaneous activity in white-matter networks

To further investigate the spontaneous activity of white-matter

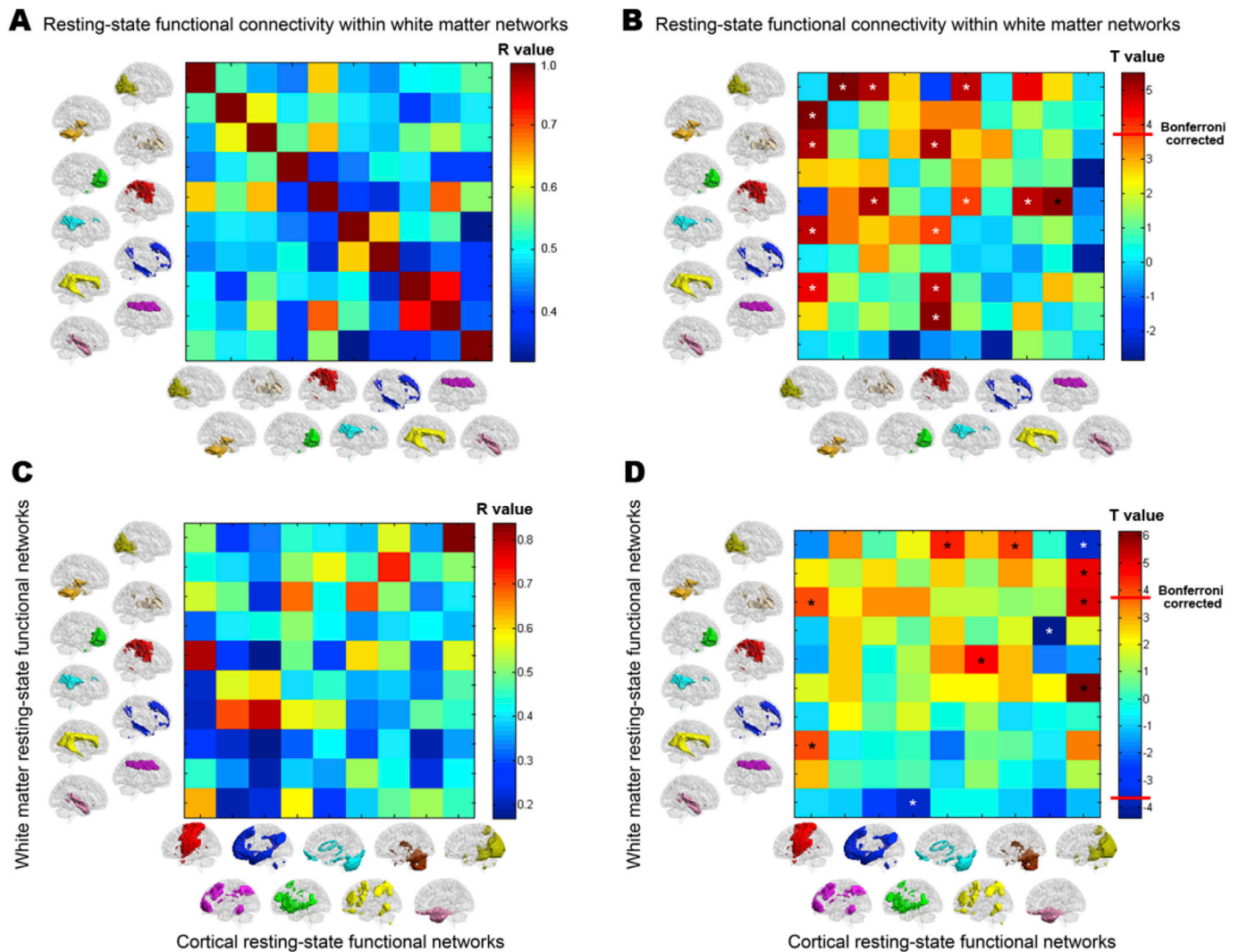


Fig. 2. Functional connectivity of white-matter networks in the resting-state. (A) Average functional connectivity strength between the different white-matter networks. The color bar shows the correlation coefficient (i.e., R value). (B) Differences in functional connectivity within the white-matter networks between schizophrenia patients and healthy controls. The color bar shows the T value from the two-sample t-tests. * represents significant differences after Bonferroni correction. (C) Average functional connectivity strength between white-matter networks and gray-matter networks. The color bar shows the correlation coefficient (i.e., R value). (D) Differences in the functional connectivity of white-matter and gray-matter networks between schizophrenia patients and healthy controls. The color bar shows the T value from the two-sample t-tests. * represents significant differences after Bonferroni correction.

networks, Fourier transform was performed on the signals from white-matter networks. All the white-matter networks showed a gradual decrease in amplitude with increased frequency, which indicated greater

Table 2
Increased functional connectivity between distinct white-matter networks in patients with schizophrenia.

White-matter network	White-matter network	T value	P value
Occipital network	Cerebellar network	5.51	1.0×10^{-7}
	Anterior corona radiate network	5.11	7.1×10^{-7}
	Posterior callosum network	4.98	1.3×10^{-6}
Pre/post-central network	Deep network	4.59	7.4×10^{-6}
	Anterior corona radiate network	5.07	8.6×10^{-7}
	Posterior callosum network	3.82	1.7×10^{-4}
	Deep network	4.89	2.0×10^{-6}
	Superior corona radiate network	5.38	1.9×10^{-7}

Table 3
Altered functional connectivity between white-matter and gray-matter networks in patients with schizophrenia.

White-matter network	Gray-matter network	T value	P value
Occipital network	Cerebellum posterior network	4.49	1.2×10^{-5}
	Cerebellum anterior network	4.09	6.0×10^{-5}
	Visual network	-3.65	3.3×10^{-4}
Cerebellar network	Visual network	4.95	1.5×10^{-6}
	Sensori-motor network	4.01	8.5×10^{-5}
Anterior corona radiate network	Visual network	5.11	7.3×10^{-7}
Orbitofrontal network	Temporal-orbitofrontal network	-4.38	1.9×10^{-5}
Pre/post-central network	Dorsal attention network	4.80	2.9×10^{-6}
Posterior callosum network	Visual network	6.18	3.2×10^{-9}
Deep network	Sensori-motor network	4.00	8.6×10^{-5}
Superior temporal network	Ventral attention network	-3.64	3.4×10^{-4}

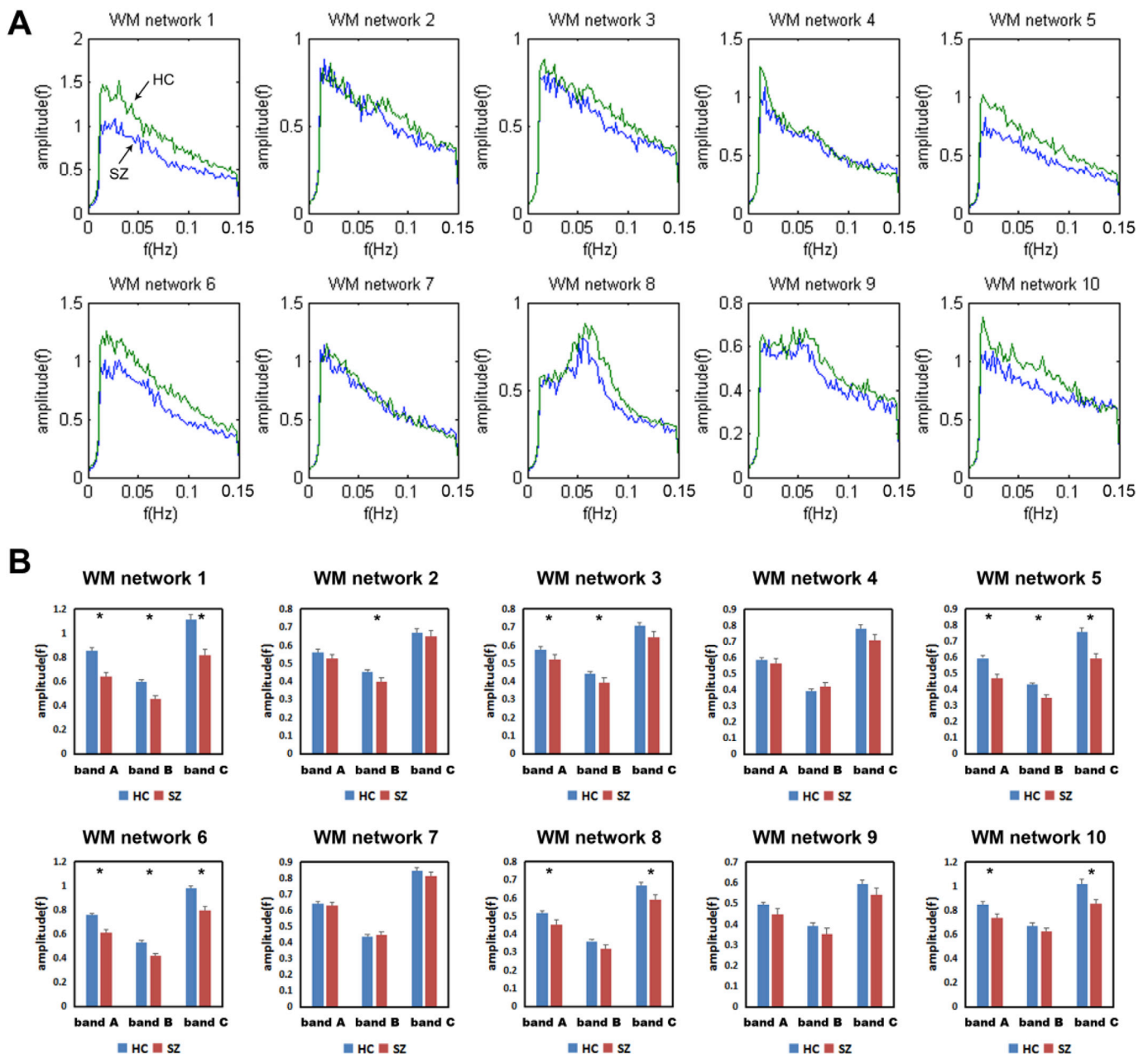


Fig. 3. Spontaneous activity of white-matter networks in the resting-state. Power spectral analysis was performed on signals in the white-matter networks. (A) Power-frequency graphs for the ten white-matter networks. WM, white-matter; HC, healthy controls; SZ, schizophrenia. (B) Differences in the average amplitude in different frequency bands between schizophrenia patients and healthy controls. Band A: 0.01–0.15 Hz; band B: 0.08–0.15 Hz; band C: 0.01–0.08 Hz * represents the significant differences by ANOVA.

activity at low frequencies (Fig. 3a). Our findings supported a prior opinion that BOLD signals at low frequencies reflect spontaneous neural activity. In addition, we found distinct spontaneous activity patterns between the superficial and deep white-matter networks. In particular, the superficial white-matter networks exhibited maximal activity at the lowest frequency 0.01 Hz, whereas the deep networks showed a maximal amplitude at 0.07 Hz (Fig. 3a).

To examine the differences in spontaneous white-matter neural activity between the schizophrenia and healthy control groups, we did comparisons using ANOVA. Comparisons showed that the amplitudes at the low frequency (band C) were decreased in white-matter 1, 5, 6, 8 and 10 in the schizophrenia group (Fig. 3b). The amplitudes at the high frequency (band B) were decreased in white-matter 1, 2, 3, 5 and 6 in the schizophrenia group (Fig. 3b). The details are provided in Supplementary 7.

Correlations between altered white-matter networks and clinical variables

Correlation analyses found that three white-matter functional connections (white-matter networks 1 and 8, 5 and 8, and 5 and 9) were positively associated with disease duration. Moreover, one white-matter and gray-matter functional connection (white-matter network 8 and gray-matter sensori-motor network) was positively correlated with disease duration. In addition, the low frequency spontaneous fluctuations of white-matter networks 6, 8 and 10 were negatively associated with disease duration. The results can be seen in Fig. 4 and Supplementary 8. In addition, the PANSS score and anti-psychotic medications showed no association with white-matter functional index.

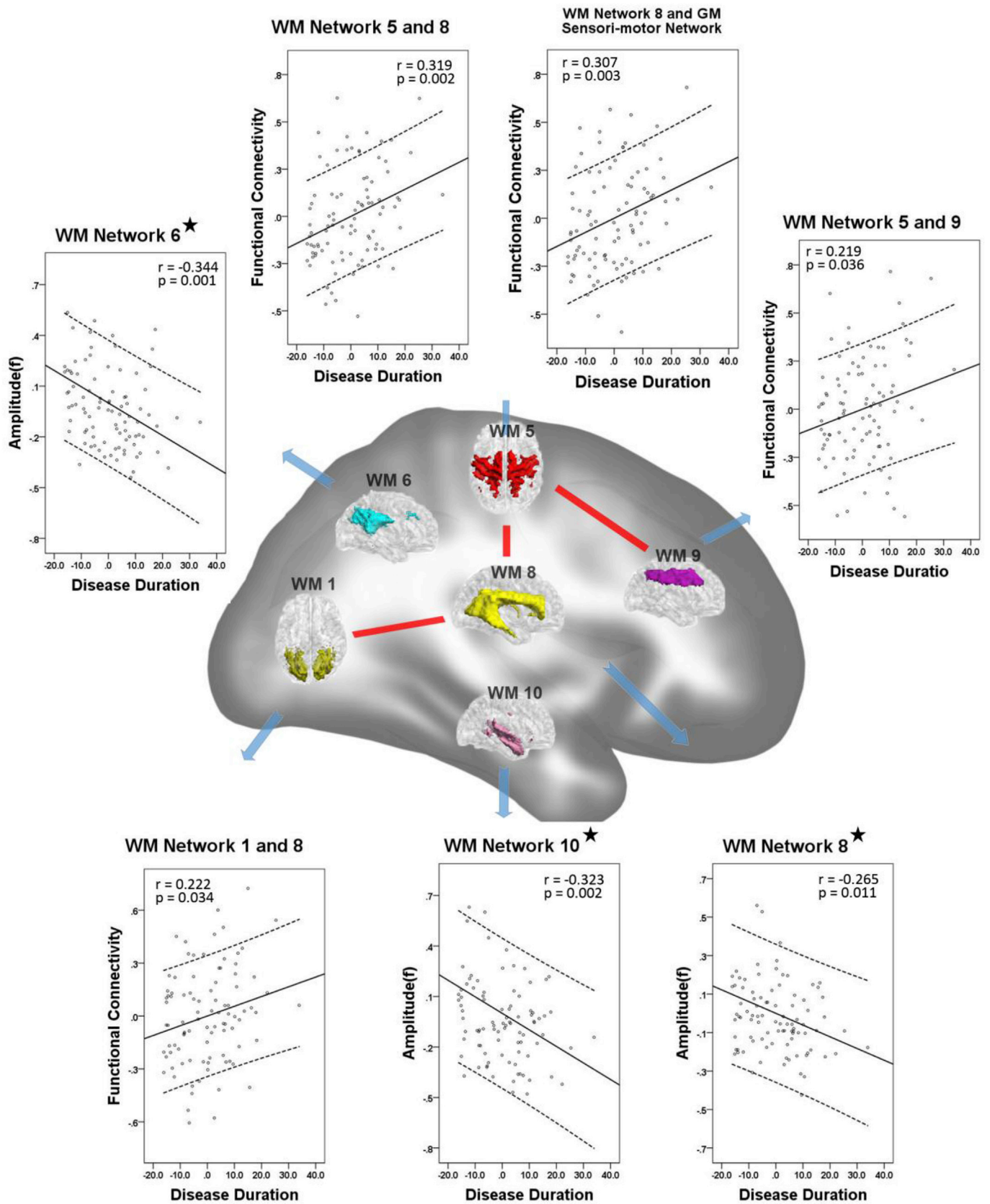


Fig. 4. Correlations between altered white-matter networks and disease duration. Three white-matter functional connections (white-matter network 1 and 8, 5 and 8, and 5 and 9) were positively associated with disease duration. One white-matter and gray-matter functional connection (white-matter network 8 and gray-matter sensori-motor network) was positively correlated with disease duration. The low frequency spontaneous fluctuations of white-matter networks 6, 8 and 10 were negatively associated with disease duration. The star represents that outliers ($> \text{mean} \pm 2 \times \text{SD}$) dots were removed from these scatter diagrams (two dots in WM6, one dot in WM8, and three dots in WM10).

Potential influences of gray-matter signals

To eliminate potential interference from neighboring gray-matter, we applied two stricter masks (percentages >70% and >80%) for white-matter. We found that the results from 70% to 80% masks were consistent with the results of the 60% mask, and the high correlation coefficient between the results using the 60% mask and that of the stricter masks indicated that the results remained stable even with a stricter mask (Supplementary 2). In addition, gray-matter signal regression reduced the correlation between white-matter clusters and induced a negative correlation, but it did not alter the relative connectivity strength or influence the comparisons between the patients and healthy controls (Supplementary 4). Finally, in most of the white-matter networks, the significant correlations with the gray-matter network were not associated with their spatial distance (Supplementary 5).

Discussion

Consistent with a previous study (Peer et al., 2017), this study showed that distinct white-matter functional networks could be identified using correlation analysis of resting-state fMRI signals. By evaluating the spontaneous activities and functional connectivity within the white-matter, schizophrenia patients illustrated the decreased amplitude of low-frequency oscillation and increased functional connectivity in superficial perception-motor white-matter networks, suggesting the abnormality of perception-motor system in schizophrenia from the perspective of white-matter functional networks. Additionally, the superficial perception-motor white-matter networks had decreased functional connectivity with cortical perception-motor gray-matter networks (close-range communication). In contrast, the middle and deep white-matter networks had increased functional connectivity with the superficial perception-motor white-matter networks and cortical perception-motor gray-matter networks (long-range communication). The disrupted association between the gray-matter and white-matter networks in the perception-motor system might be compensated through the middle-deep white-matter networks. This may be the foundation of extensive disrupted connections among brain regions in schizophrenia. Finally, the deep white-matter network representing the primary fiber tracts exhibited some significant alterations that were associated with illness duration in schizophrenia.

In general, the BOLD signals observed in the gray-matter reflect the activity of the neurons. Task-related fMRI, however, has illustrated activation inside the white-matter (Fabri and Polonara, 2013; Gawryluk et al., 2014; Mazerolle et al., 2008). A recent study has reported that using fMRI signals, white-matter voxels can be clustered into several networks according to their functional connectivity pattern (Peer et al.,

2017). Here, we identified ten white-matter functional networks consisting of three layers (superficial, middle and deep). Most of the superficial white-matter networks were correlated with their overlying gray-matter networks, whereas the deep network had a relatively weak association with all the gray-matter networks. Similar to the gray-matter networks, the major amplitudes of low frequency fluctuations in the white-matter networks were located in the range of less than 0.1 Hz. These features of white-matter networks can provide additional information for investigating the differences between health and disease.

Previous studies have reported the decreased BOLD signal amplitude at low-frequency in perception-motor gray-matter networks in schizophrenia (Alonso-Solis et al., 2017; Hoptman et al., 2010; Meda et al., 2015). The current study also observed a decreased BOLD amplitude at low frequencies in three superficial white-matter networks (visual, temporal and sensori-motor). In addition, previous studies have indicated that a mismatch between visual and sensori-motor signals is sufficient to induce self-related disturbances in patients with schizophrenia (Ehrsson, 2007). We also observed increased functional connectivity between the superficial white-matter networks (visual and sensori-motor) and the middle/deep white-matter networks. This enhanced functional connectivity may suggest an insufficient or ineffective communication in the white-matter and may be a possible fundamental mechanism that explains the perception-motor processing deficits in patients with schizophrenia. Furthermore, these increases in functional connection were also associated with disease duration, which provided evidence that progressive abnormality of functional integrations occurred within white-matter networks.

In addition, the informational interaction between white-matter and gray-matter networks may have two transmission pathways: close-range and long-range communications. Both of these are altered in schizophrenia patients: close-range communication is decreased, but long-range communication is increased. In detail, the white-matter visual, orbitofrontal and temporal networks had decreased functional connectivity with their overlying gray-matter networks (close-range communication). In contrast, the middle and deep white-matter networks had increased functional connectivity with the visual and motor gray-matter networks (long-range communication). Therefore, it can be hypothesized that the disrupted association between the gray-matter and white-matter networks in the perception-motor system may be compensated for through the middle-deep white-matter networks (Fig. 5).

In this study, the deep white-matter network covered the major association fiber tracts, including the superior longitudinal fasciculus and the inferior longitudinal fasciculus, which are considered to be the fundamental link between lobes within hemispheres. Different from the other white-matter networks, the deep network exhibited some unique features. Compared to the other white-matter networks, the deep

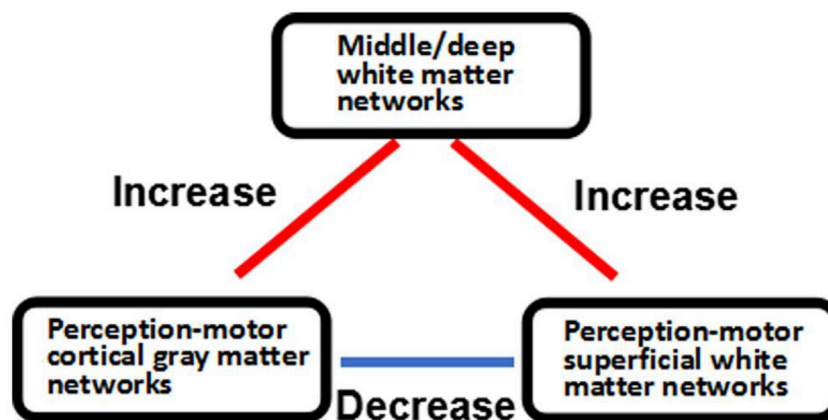


Fig. 5. A possible compensatory mechanism in schizophrenia. The disrupted association between cortical gray-matter and superficial white-matter networks in the perception-motor system may be compensated for through the middle-deep white-matter networks.

network had weaker correlations with all the gray-matter networks. In addition, it showed a maximal resting state activity at a relatively high frequency of 0.07 Hz. To explain this phenomenon, Peer et al. suggested that the deep network might have specific functions other than the typical functions of gray-matter networks (Peer et al., 2017). Moreover, compared with healthy controls, we observed decreased amplitude of low-frequency oscillation in the deep network in schizophrenia. Furthermore, the greater decrease in amplitude in the deep network was linked to longer disease duration. In addition, we observed reduced amplitude of low-frequency oscillation in the middle white-matter network, the posterior callosum network, which is mainly composed of posterior callosum, posterior cingulate and precuneus regions. The reduced amplitude of low-frequency oscillations in these regions has been widely reported (Meda et al., 2015). These findings provided additional evidence that there is an abnormality of the primary fibers that are part of the deep white-matter network in schizophrenia. These changes were consistent with previous DTI studies (Dong et al., 2017a; Lener et al., 2015; Park et al., 2004).

This study should be interpreted with caution because of several limitations. First, there is doubt as to whether the observed white-matter signals reflect neuron-related activity, since the white-matter had very few postsynaptic potentials that gave rise to BOLD signals (Logothetis et al., 2001). Previous studies put forward two possible sources for white-matter BOLD signals: spiking-related metabolic demands and astrocytes and NO-producing neurons activity (Gawryluk et al., 2014). The contribution of blood vessels across the white-matter may also be a reason (Gawryluk et al., 2014). In addition, as white-matter tracts cross each other, the same white-matter locations may mix signals from different functional systems. Therefore, it is difficult to say where the precise source of the fMRI signals is in the white-matter. Although we cannot clarify the source of white-matter functional activity, we found that the signals from white-matter share common and typical characteristics with those of gray-matter. These signals of white-matter can add an additional layer of information regarding differences between health and diseases. Another issue is the possible attribution of gray-matter signals to white-matter due to partial-volume effects. This problem can be exacerbated by spatial smoothing. By smoothing the white-matter and gray-matter separately and using only the voxels that were identified as white-matter from each subject, we took measures as early as possible to ensure that the gray-matter signals did not interfere with the white-matter signals. These measures, together with the finding of an association between disease duration and the amplitude of low frequency oscillation in the deep network, might reflect an alteration related with the white-matter in schizophrenia. However, this partial volume effect is only partially addressed by segmentation of the white-matter and gray-matter. The fMRI signal within a voxel is not independent from that of its neighbors due to BOLD-image reconstruction and the underlying physiological (vascular) and physical (MRI) effects. It is thus always of concern whether or not the correlation or clustering pattern of white-matter fMRI signals are simply due to the leakage of the gray-matter fMRI signals. To our knowledge, it is difficult to eliminate this problem by using the standard data acquisition sequence/parameters. In addition, some artifacts, such as respiration, head motion and scanner noise, may contaminate the white-matter signals. In general, the foundations of white-matter fMRI are not established at this stage, and future work should address these methodological issues. Most of the schizophrenia patients in this study had chronic schizophrenia and received antipsychotic medications. Their clinical symptoms were in stable condition and appeared to be under control, which may be the reason why no correlation was observed between the white-matter functional connectivity and the clinical symptoms. Thus, first-episode, drug-naïve schizophrenia patients would need to be included to further assess the correlation between white-matter functional connectivity and clinical symptoms in the future. In addition, neuropsychological tests and cognitive measures were not included in this study; thus, we could not assess the association between cognitive and brain changes. Finally, it

was impossible to exclude random bias in this observational study.

Conclusions

The present study demonstrated the perception-motor system changes in schizophrenia from the viewpoint of white-matter functional networks. In addition, this study uncovered aberrant interactions between the superficial white-matter networks and cortical gray-matter networks. The disrupted association between the gray-matter and superficial white-matter networks in perception-motor system might be compensated for through the middle-deep white-matter networks, suggesting a possible fundamental mechanism that underlies the extensive disrupted connections among brain regions in schizophrenia. Finally, the deep white-matter network exhibited some specific alterations that provided additional information for understanding the abnormalities in primary fibers in schizophrenia.

Declarations of interest

None.

Acknowledgements

This study was supported by the National Nature Science Foundation of China (No. 81330032, 81471638, 81571759, 81771822), Sichuan Province Science and Technology Support Project (No.2017SZ0004), the“111” Project (B12027) and the Chinese Fundamental Research Funding for Central Universities in UESTC (ZYGX2016J121, ZYGX2016J124).

Appendix A. Supplementary data

Supplementary data related to this article can be found at <https://doi.org/10.1016/j.neuroimage.2018.04.018>.

References

- Alonso-Solis, A., Vives-Gilabert, Y., Portella, M.J., Rabella, M., Grasa, E.M., Roldan, A., Keymer-Gausset, A., Molins, C., Nunez-Marin, F., Gomez-Anson, B., Alvarez, E., Corripio, I., 2017. Altered amplitude of low frequency fluctuations in schizophrenia patients with persistent auditory verbal hallucinations. *Schizophr. Res.*
- Biswal, B., Yetkin, F.Z., Haughton, V.M., Hyde, J.S., 1995. Functional connectivity in the motor cortex of resting human brain using echo-planar MRI. *Magn. Reson. Med.* 34, 537–541.
- Bohnen, N.L., Albin, R.L., 2011. White matter lesions in Parkinson disease. *Nat. Rev. Neurol.* 7, 229–236.
- Buchsbaum, M.S., Buchsbaum, B.R., Hazlett, E.A., Haznedar, M.M., Newmark, R., Tang, C.Y., Hof, P.R., 2007. Relative glucose metabolic rate higher in white matter in patients with schizophrenia. *Am. J. Psychiatry* 164, 1072–1081.
- Buckner, R.L., Krienen, F.M., Castellanos, A., Diaz, J.C., Yeo, B.T., 2011. The organization of the human cerebellum estimated by intrinsic functional connectivity. *J. Neurophysiol.* 106, 2322–2345.
- Burns, J., Job, D., Bastin, M.E., Whalley, H., Macgillivray, T., Johnstone, E.C., Lawrie, S.M., 2003. Structural disconnectivity in schizophrenia: a diffusion tensor magnetic resonance imaging study. *Br. J. Psychiatry* 182, 439–443.
- Caso, F., Agosta, F., Mattavelli, D., Migliaccio, R., Canu, E., Magnani, G., Marcone, A., Copetti, M., Falautano, M., Comi, G., Falini, A., Filippi, M., 2015. White matter degeneration in atypical alzheimer disease. *Radiology* 277, 162–172.
- Chen, X., Jiang, Y., Chen, L., He, H., Dong, L., Hou, C., Duan, M., Yang, M., Yao, D., Luo, C., 2017. Altered hippocampo-cerebello-cortical circuit in schizophrenia by a spatiotemporal consistency and causal connectivity analysis. *Front. Neurosci.* 11, 25.
- Craddock, R.C., James, G.A., Holtzheimer, P.E., Hu, X.P.P., Mayberg, H.S., 2012. A whole brain fMRI atlas generated via spatially constrained spectral clustering. *Hum. Brain Mapp.* 33, 1914–1928.
- Desikan, R.S., Segonne, F., Fischl, B., Quinn, B.T., Dickerson, B.C., Blacker, D., Buckner, R.L., Dale, A.M., Maguire, R.P., Hyman, B.T., Albert, M.S., Killiany, R.J., 2006. An automated labeling system for subdividing the human cerebral cortex on MRI scans into gyral based regions of interest. *Neuroimage* 31, 968–980.
- Ding, Z.H., Huang, Y.L., Bailey, S.K., Gao, Y.R., Cutting, L.E., Rogers, B.P., Newton, A.T., Gore, J.C., 2018. Detection of synchronous brain activity in white matter tracts at rest and under functional loading. *Proc. Natl. Acad. Sci. U. S. A.* 115, 595–600.
- Dong, D., Wang, Y., Chang, X., Jiang, Y., Klugah-Brown, B., Luo, C., Yao, D., 2017a. Shared abnormality of white matter integrity in schizophrenia and bipolar disorder: a comparative voxel-based meta-analysis. *Schizophr. Res.*

- Dong, D., Wang, Y., Chang, X., Luo, C., Yao, D., 2017b. Dysfunction of large-scale brain networks in schizophrenia: a meta-analysis of resting-state functional connectivity. *Schizophr. Bull.*
- Duan, M., Chen, X., He, H., Jiang, Y., Jiang, S., Xie, Q., Lai, Y., Luo, C., Yao, D., 2015. Altered basal ganglia network integration in schizophrenia. *Front. Hum. Neurosci.* 9, 561.
- Ehrsson, H.H., 2007. The experimental induction of out-of-body experiences. *Science* 317, 1048.
- Fabri, M., Polonara, G., 2013. Functional topography of human corpus callosum: an fMRI mapping study. *Neural Plast.* 2013, 251308.
- Fabri, M., Polonara, G., Mascioli, G., Salvolini, U., Manzoni, T., 2011. Topographical organization of human corpus callosum: an fMRI mapping study. *Brain Res.* 1370, 99–111.
- Fox, M.D., Raichle, M.E., 2007. Spontaneous fluctuations in brain activity observed with functional magnetic resonance imaging. *Nat. Rev. Neurosci.* 8, 700–711.
- Friston, K.J., 1998. The disconnection hypothesis. *Schizophr. Res.* 30, 115–125.
- Gawryluk, J.R., Mazerolle, E.L., Brewer, K.D., Beyea, S.D., D'Arcy, R.C., 2011. Investigation of fMRI activation in the internal capsule. *BMC Neurosci.* 12, 56.
- Gawryluk, J.R., Mazerolle, E.L., D'Arcy, R.C., 2014. Does functional MRI detect activation in white matter? A review of emerging evidence, issues, and future directions. *Front. Neurosci.* 8, 239.
- Holleran, L., Ahmed, M., Anderson-Schmidt, H., McFarland, J., Emsell, L., Leemans, A., Scanlon, C., Dockery, P., McCarthy, P., Barker, G.J., McDonald, C., Cannon, D.M., 2014. Altered interhemispheric and temporal lobe white matter microstructural organization in severe chronic schizophrenia. *Neuropsychopharmacology* 39, 944–954.
- Hoptman, M.J., Zuo, X.N., Butler, P.D., Javitt, D.C., D'Angelo, D., Mauro, C.J., Milham, M.P., 2010. Amplitude of low-frequency oscillations in schizophrenia: a resting state fMRI study. *Schizophr. Res.* 117, 13–20.
- Huang, H., Jiang, Y., Xia, M., Tang, Y., Zhang, T., Cui, H., Wang, J., Li, Y., Xu, L., Curtin, A., Sheng, J., Jia, Y., Yao, D., Li, C., Luo, C., Wang, J., 2017. Increased resting-state global functional connectivity density of default mode network in schizophrenia subjects treated with electroconvulsive therapy. *Schizophr. Res.*
- Ji, G.J., Liao, W., Chen, F.F., Zhang, L., Wang, K., 2017. Low-frequency blood oxygen level-dependent fluctuations in the brain white matter: more than just noise. *Sci. Bull.* 62, 656–657.
- Jiang, Y., Duan, M., Chen, X., Chang, X., He, H., Li, Y., Luo, C., Yao, D., 2017. Common and distinct dysfunctional patterns contribute to triple network model in schizophrenia and depression: a preliminary study. *Prog. Neuropsychopharmacol. Biol. Psychiatry* 79, 302–310.
- Jiang, Y., Luo, C., Li, X., Duan, M., He, H., Chen, X., Yang, H., Gong, J., Chang, X., Woelfer, M., Biswal, B.B., Yao, D., 2018. Progressive reduction in gray matter in patients with schizophrenia assessed with MR imaging by using causal network analysis. *Radiology* 0, 171832.
- Karlsgodt, K.H., van Erp, T.G., Poldrack, R.A., Bearden, C.E., Nuechterlein, K.H., Cannon, T.D., 2008. Diffusion tensor imaging of the superior longitudinal fasciculus and working memory in recent-onset schizophrenia. *Biol. Psychiatry* 63, 512–518.
- Kressel, H.Y., 2017. Setting sail: 2017. *Radiology* 282, 4–6.
- Lener, M.S., Wong, E., Tang, C.Y., Byne, W., Goldstein, K.E., Blair, N.J., Haznedar, M.M., New, A.S., Chmerinski, E., Chu, K.W., Rimsky, L.S., Siever, L.J., Koeningberg, H.W., Hazlett, E.A., 2015. White matter abnormalities in schizophrenia and schizotypal personality disorder. *Schizophr. Bull.* 41, 300–310.
- Logothetis, N.K., Pauls, J., Augath, M., Trinath, T., Oeltermann, A., 2001. Neurophysiological investigation of the basis of the fMRI signal. *Nature* 412, 150–157.
- Lorio, S., Fresard, S., Adaszewski, S., Kherif, F., Chowdhury, R., Frackowiak, R.S., Ashburner, J., Helms, G., Weiskopf, N., Lutti, A., Draganski, B., 2016. New tissue priors for improved automated classification of subcortical brain structures on MRI. *Neuroimage* 130, 157–166.
- Lui, S., Zhou, X.J., Sweeney, J.A., Gong, Q., 2016. Psychoradiology: the frontier of neuroimaging in psychiatry. *Radiology* 281, 357–372.
- Marussich, L., Lu, K.H., Wen, H., Liu, Z., 2017. Mapping white-matter functional organization at rest and during naturalistic visual perception. *Neuroimage* 146, 1128–1141.
- Mazerolle, E.L., D'Arcy, R.C., Beyea, S.D., 2008. Detecting functional magnetic resonance imaging activation in white matter: interhemispheric transfer across the corpus callosum. *BMC Neurosci.* 9, 84.
- Meda, S.A., Ruano, G., Windemuth, A., O'Neil, K., Berwise, C., Dunn, S.M., Boccaccio, L.E., Narayanan, B., Kocherla, M., Sprooten, E., Keshavan, M.S., Tamminga, C.A., Sweeney, J.A., Clementz, B.A., Calhoun, V.D., Pearlson, G.D., 2014. Multivariate analysis reveals genetic associations of the resting default mode network in psychotic bipolar disorder and schizophrenia. *Proc. Natl. Acad. Sci. U. S. A.* 111, E2066–E2075.
- Meda, S.A., Wang, Z., Ivleva, E.I., Poudyal, G., Keshavan, M.S., Tamminga, C.A., Sweeney, J.A., Clementz, B.A., Schretlen, D.J., Calhoun, V.D., Lui, S., Damaraju, E., Pearlson, G.D., 2015. Frequency-specific neural signatures of spontaneous low-frequency resting state fluctuations in psychosis: evidence from bipolar-schizophrenia network on intermediate phenotypes (B-SNIP) consortium. *Schizophr. Bull.* 41, 1336–1348.
- Mezer, A., Yovel, Y., Pasternak, O., Gorfine, T., Assaf, Y., 2009. Cluster analysis of resting-state fMRI time series. *Neuroimage* 45, 1117–1125.
- Park, H.J., Westin, C.F., Kubicki, M., Maier, S.E., Niznikiewicz, M., Baer, A., Frumin, M., Kikinis, R., Jolesz, F.A., McCarley, R.W., Shenton, M.E., 2004. White matter hemisphere asymmetries in healthy subjects and in schizophrenia: a diffusion tensor MRI study. *Neuroimage* 23, 213–223.
- Peer, M., Nitzan, M., Bick, A.S., Levin, N., Arzyt, S., 2017. Evidence for functional networks within the human Brain's white matter. *J. Neurosci.* 37, 6394–6407.
- Power, J.D., Cohen, A.L., Nelson, S.M., Wig, G.S., Barnes, K.A., Church, J.A., Vogel, A.C., Laumann, T.O., Miezin, F.M., Schlaggar, B.L., Petersen, S.E., 2011. Functional network organization of the human brain. *Neuron* 72, 665–678.
- Shirer, W.R., Ryali, S., Rykhlevskaia, E., Menon, V., Greicius, M.D., 2012. Decoding subject-driven cognitive states with whole-brain connectivity patterns. *Cereb. Cortex* 22, 158–165.
- Smith, S.M., Jenkinson, M., Johansen-Berg, H., Rueckert, D., Nichols, T.E., Mackay, C.E., Watkins, K.E., Ciccarelli, O., Cader, M.Z., Matthews, P.M., Behrens, T.E., 2006. Tract-based spatial statistics: voxelwise analysis of multi-subject diffusion data. *Neuroimage* 31, 1487–1505.
- Xue, K., Luo, C., Zhang, D., Yang, T., Li, J., Gong, D., Chen, L., Medina, Y.I., Gotman, J., Zhou, D., Yao, D., 2014. Diffusion tensor tractography reveals disrupted structural connectivity in childhood absence epilepsy. *Epilepsy Res.* 108, 125–138.
- Yeo, B.T.T., Krienen, F.M., Sepulcre, J., Sabuncu, M.R., Lashkari, D., Hollinshead, M., Roffman, J.L., Smoller, J.W., Zoller, L., Polimeni, J.R., Fischl, B., Liu, H.S., Buckner, R.L., 2011. The organization of the human cerebral cortex estimated by intrinsic functional connectivity. *J. Neurophysiol.* 106, 1125–1165.
- Yu, R., Chien, Y.L., Wang, H.L., Liu, C.M., Liu, C.C., Hwang, T.J., Hsieh, M.H., Hwu, H.G., Tseng, W.Y., 2014. Frequency-specific alternations in the amplitude of low-frequency fluctuations in schizophrenia. *Hum. Brain Mapp.* 35, 627–637.